CHAPTER 4

FLEXURAL STRENGTHENING OF REINFORCED CONCRETE

4.1 General

Reinforced concrete members, such as beams and columns, may be strengthened in flexure through the use of strips or sheets epoxy-bonded to their tension zones, with the direction of fibers parallel to that of high tensile stresses (member axis). The concept is illustrated in Fig. 4.1. Flexural strengthening of columns is, in general, more difficult to achieve, due to the requirements for anchorage of the FRP through the joints. The latter is easy to construct if the width of beams is smaller than that of columns (hence sufficient space is available to bond strips, Fig. 4.2b), but requires small FRP cross sections placed near the column corners if the column and the beams have similar dimensions (Fig. 4.2c).

The analysis for the ultimate limit state in flexure may follow well-established procedures for reinforced concrete structures, provided that: (a) the contribution of external FRP reinforcement is taken into account properly (linear elastic material); and (b) special consideration is given to the issue of bond between the concrete and the FRP.

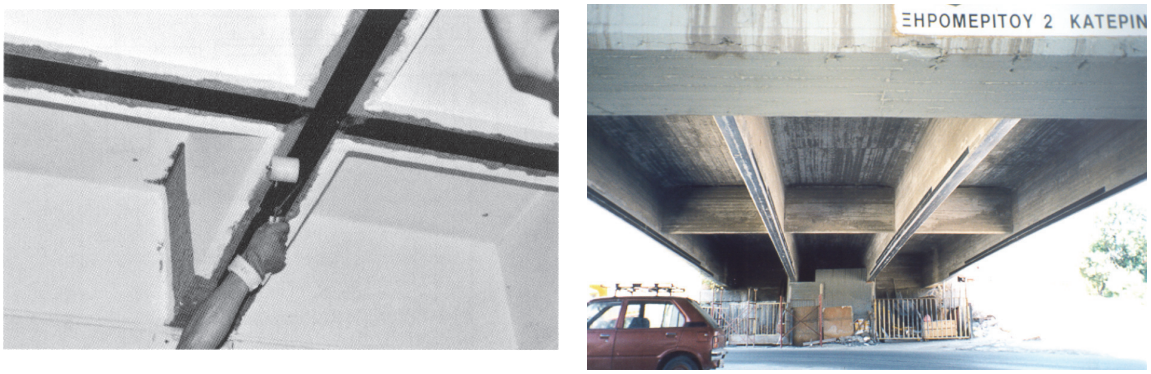

Fig. 4.1 Flexural strengthening of beams.

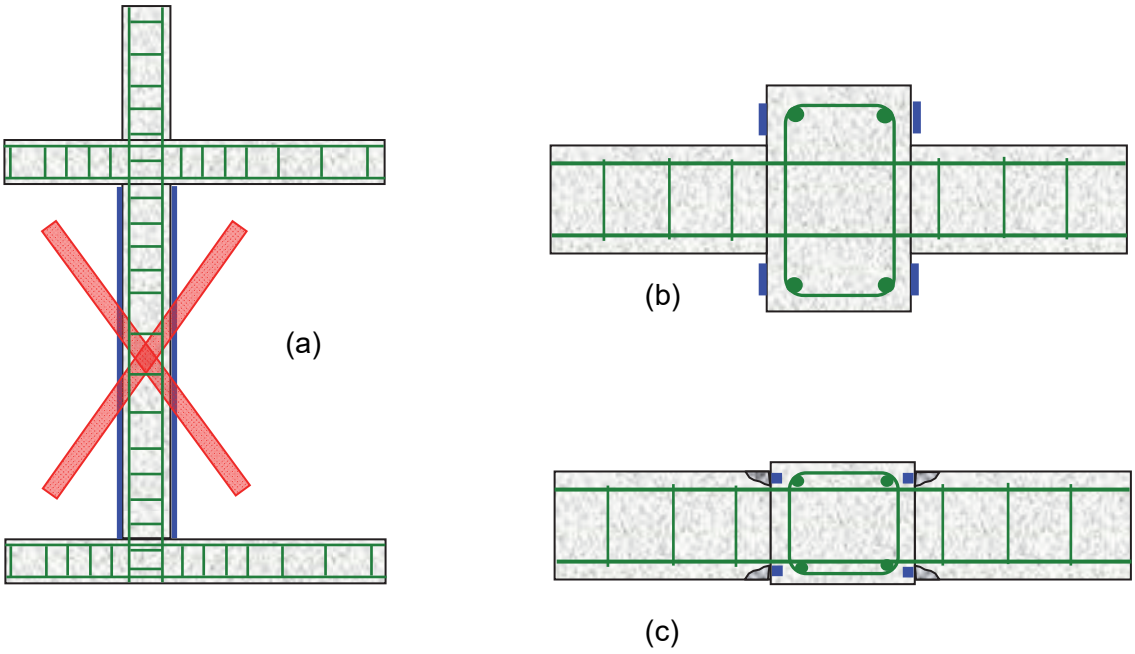

Fig. 4.2 Flexural strengthening of columns with maximum moment at the ends requires proper anchorage of the external reinforcement. (a) Incorrect application, (b) continuity of the FRP through the slab, (c) continuity of the FRP through the joint.

4.2 Initial situation

The effect of the initial load prior to strengthening should be considered in the calculation of the strengthened member. Based on the theory of elasticity and with M_o the service moment (no load safety factors are applied) acting on the critical RC section during strengthening, the strain distribution of the member can be evaluated. As M_o is typically larger than the cracking moment M_{cr}, the calculation is based on a cracked section (Fig. 4.3). If M_o is smaller than M_{cr}, its influence on the calculation of the strengthened member may easily be neglected.

Based on the transformed cracked section, the neutral axis depth x_o can be solved from:

$$\frac{1}{2}bx_o^2 + (\alpha_s - 1)A_{s2}(x_o - d_2) = \alpha_s A_{s1}(d - x_o) \qquad (4.1)$$

where A_{s1} = area of tension steel, A_{s2} = area of compression steel, d_1 = distance of tension steel centroid to extreme tension fiber, d_2 = distance of compression steel centroid to extreme compression fiber, d = static depth, h = height of cross section, b = width of cross section and $\alpha_s = E_s / E_c$ = ratio of steel elastic modulus to concrete elastic modulus. The concrete strain ε_{co} at the extreme compression fiber is calculated as follows:

$$\varepsilon_{co} = \frac{M_o x_o}{E_c I_{o2}} \tag{4.2}$$

where I_{o2} is the moment of inertia of the transformed cracked section:

$$I_{o2} = \frac{b x_o^3}{3} + (\alpha_s - 1) A_{s2} (x_o - d_2)^2 + \alpha_s A_{s1} (d - x_o)^2 \tag{4.3}$$

Based on strain compatibility, the strain ε_o at the extreme tension fiber can be derived as follows:

$$\varepsilon_o = \varepsilon_{co} \frac{h - x_o}{x_o} \tag{4.4}$$

The strain ε_o determined by eq. (4.4) is the initial strain at the level of FRP when strengthening takes place.

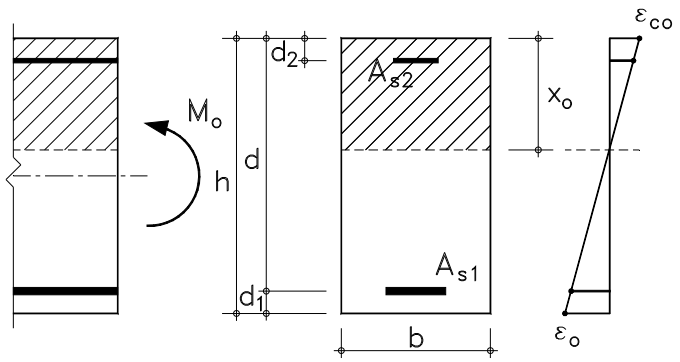

Fig. 4.3 Strain distribution in rectangular cross section subjected to moment M_o at the time of strengthening.

4.3 Ultimate limit state – failure modes

The failure mechanisms of RC members strengthened with FRP in flexure are described schematically in Fig. 4.4 (Triantafillou and Plevris 1992, Matthys 2000, *fib* 2001, Teng et al. 2001). Calculations for each failure mechanism are given in the following section.

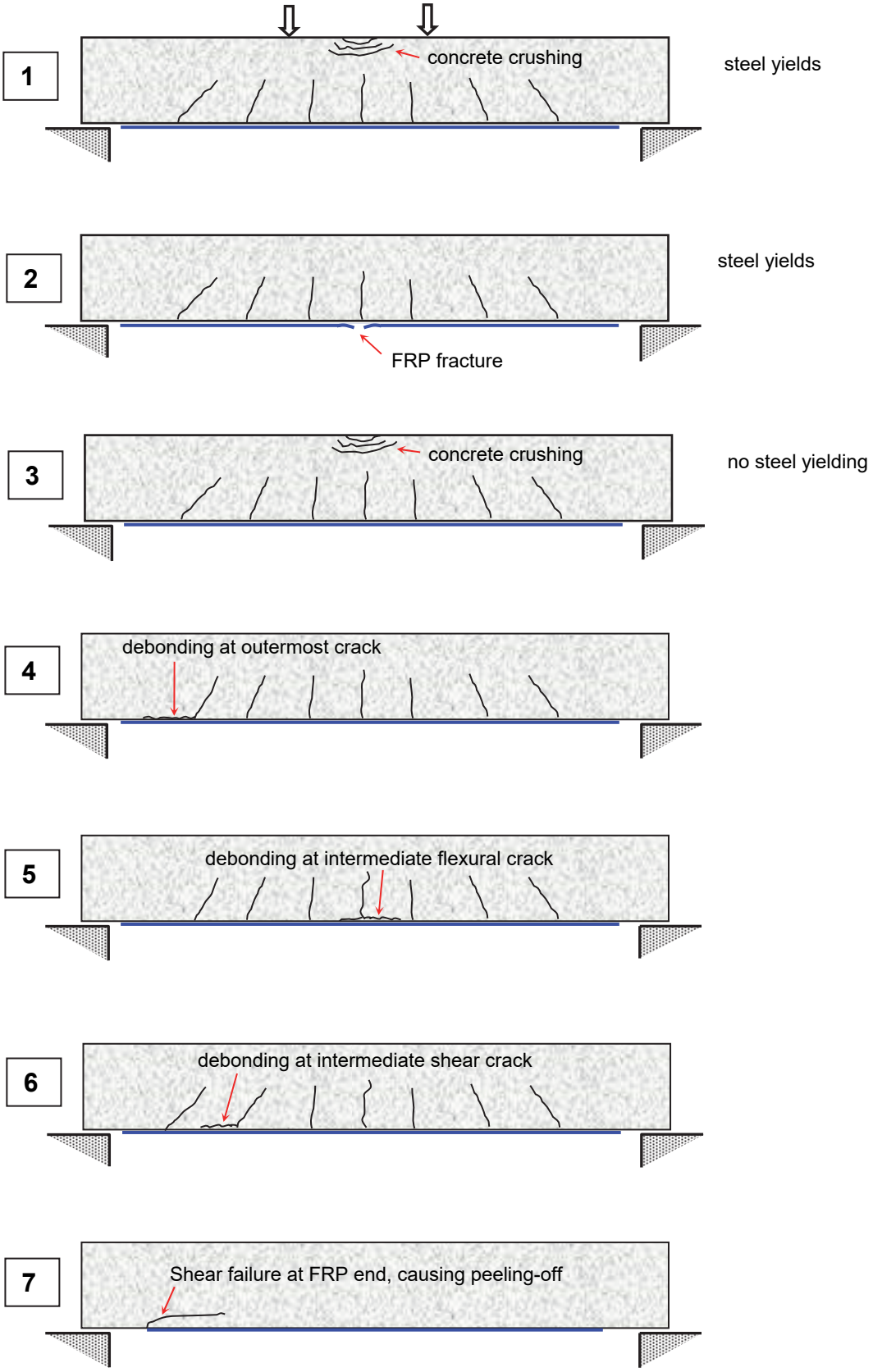

Fig. 4.4 Failure mechanisms for RC beam strengthened in flexure.

4.4 Ultimate limit state - calculations

Mechanisms (1), (2) and (3) in Fig. 4.4 are based on composite action between concrete and FRP and can be analyzed using standard procedures, whereas the other mechanisms involve some kind of debonding or peeling-off and will be analyzed separately.

4.4.1 Full composite action

(1) Steel yielding, concrete crushing

Yielding of the longitudinal steel reinforcement followed by crushing of the concrete in the compression zone is the most desirable failure mechanism. The design bending moment capacity may be calculated based on equilibrium and strain compatibility as follows (Fig. 4.5):

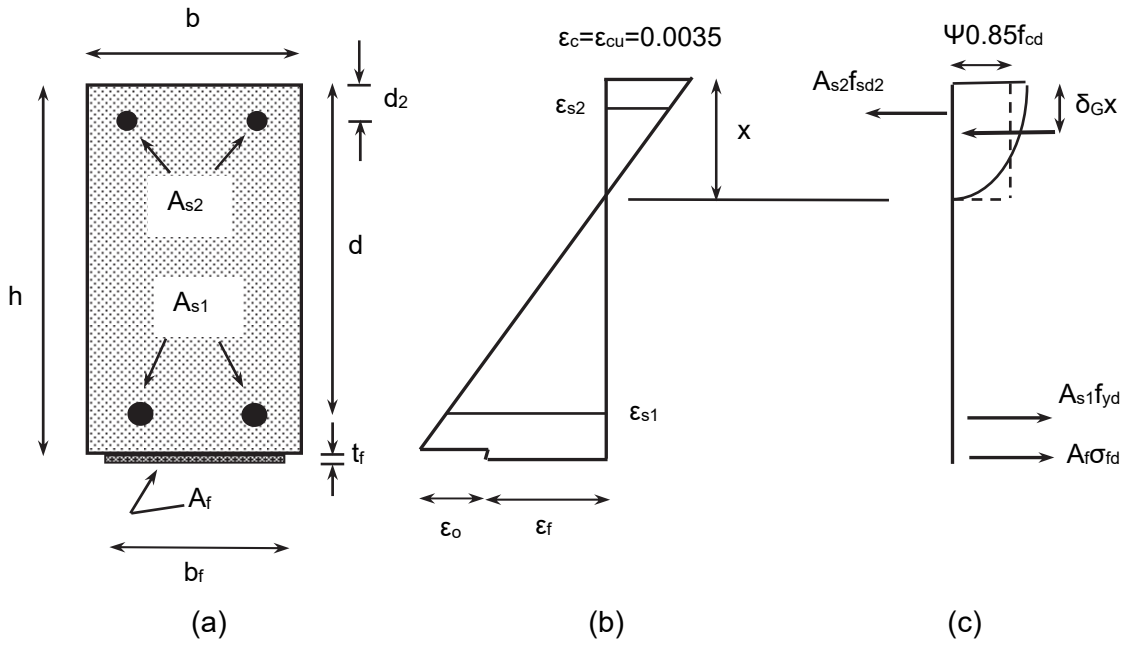

Fig. 4.5 Cross section analysis at the ultimate limit state. (a) Geometry, (b) strain distribution, (c) internal force distribution.

Calculation of neutral axis depth, x :

$$\psi 0.85 f_{cd} b x + A_{s2} f_{sd2} = A_{s1} f_{yd} + A_f \sigma_{fd} \qquad (4.5)$$

where ψ =0.8, f_{cd} = design strength of concrete, x = depth of neutral axis, f_{yd} = design value of tension steel yield stress, A_f = cross section area of FRP, f_{sd2} = design stress in

the top steel reinforcement and σ_{fd} = design stress in the FRP. Based on strain compatibility, f_{sd2} and σ_{fd} are calculated as follows:

$$f_{sd2} = E_s\left(\varepsilon_c \frac{x - d_2}{x}\right) \tag{4.6}$$

$$\sigma_{fd} = E_f\left(\varepsilon_c \frac{h - x}{x} - \varepsilon_o\right) \tag{4.7}$$

In the above expressions $\varepsilon_c = \varepsilon_{cu}$ is the ultimate strain in the concrete (=0.0035) and ε_o is the initial strain in the extreme tension fiber, given by eq. (4.4). Note that f_{sd2} should not be taken higher than f_{yd}.

Design bending moment resistance:

$$M_{Rd} = \frac{1}{\gamma_{Rd}}\left[A_{s1}f_{yd}(d - \delta_G x) + A_f\sigma_{fd}(h - \delta_G x) + A_{s2}f_{sd2}(\delta_G x - d_2)\right] \tag{4.8}$$

where δ_G=0.4, γ_{Rd} = safety factor for the calculation of the resistance in an existing member (in general $\gamma_{Rd} \geq 1$, but in the case of flexure γ_{Rd}=1).

For the equations given above to be valid, the following assumptions should be checked: (a) yielding of tensile steel reinforcement and (b) straining of the FRP is limited to the limiting strain, $\varepsilon_{f,lim}$ (corresponding to fracture or debonding):

$$\varepsilon_{s1} = \varepsilon_c \frac{d - x}{x} \geq \frac{f_{yd}}{E_s} \tag{4.9}$$

$$\varepsilon_f = \varepsilon_c \frac{h - x}{x} - \varepsilon_o \leq \varepsilon_{f,lim} \tag{4.10}$$

where $\varepsilon_c = \varepsilon_{cu}$.

(2) Steel yielding, FRP fracture

The failure mechanism involving steel yielding / FRP fracture is theoretically possible. However, it is quite likely that premature FRP debonding will precede FRP fracture and hence this mechanism will not be activated. For the sake of completeness we may state here that the analysis for this mechanism may be done along the lines of the previous section. Equations (4-5) – (4-8) still apply, with the following modifications: ε_{cu} is replaced by ε_c; σ_{fd} is replaced by f_{fde}; and ψ, δ_G are provided by the following expressions:

$$\psi = \begin{cases} 1000\varepsilon_c\left(0.5 - \dfrac{1000}{12}\varepsilon_c\right) \text{ if } \varepsilon_c \le 0.002 \\ \\ 1 - \dfrac{2}{3000\varepsilon_c} \text{ if } 0.002 \le \varepsilon_c \le 0.0035 \end{cases} \tag{4.11}$$

$$\delta_G = \begin{cases} \dfrac{8 - 1000\varepsilon_c}{4(6 - 1000\varepsilon_c)} & \text{if } \varepsilon_c \le 0.002 \\ \\ \dfrac{1000\varepsilon_c(3000\varepsilon_c - 4) + 2}{2000\varepsilon_c(3000\varepsilon_c - 2)} & \text{if } 0.002 \le \varepsilon_c \le 0.0035 \end{cases} \tag{4.12}$$

The resisting moment can be obtained by solving eqs. (4.5) – (4.8) (with the above modifications) for the three unknowns x, ε_c and M_{Rd}.

(3) Concrete crushing

Being a brittle failure mechanism, concrete crushing is not acceptable. Non-activation of this mechanism is achieved by limiting the area of FRP below certain limits. More details are provided in Section 4.5, which describes ductility requirements.

4.4.2 Loss of composite action

(4) Debonding at outermost crack

Using the analytical model described in Section 3.3 one can calculate the bond length required to prevent debonding. Consider, for example, the beam in Fig. 4.6a, with a moment diagram as shown in Fig. 4.6b (note the application of the shift rule, resulting shift of the diagram by a_ℓ). The force distribution in the tension steel (N_{sd}) and in the FRP (N_{fd}) is provided in Fig. 4.6c. As an approximation, the total tensile force (in steel and FRP), $N_{sd} + N_{fd}$, equals M_{Ed}/z, where $z = 0.95\,d$ = lever arm.

Based on Fig. 4.6c, the FRP anchorage length is calculated beyond the location (section A) where the total tension force envelope M_{Ed}/z intersects the line corresponding to the maximum force carried by the steel only, $N_{Rsd} = A_{s1}f_{yd}$. At this location the FRP tension force is N_{fad} and the corresponding anchorage length is ℓ_b. The anchorable force (design value) N_{fad} can be estimated based on internal force equilibrium as follows:

$$\frac{M_{Ed}}{z} = N_{fad}\left(1 + \frac{A_{s1}E_s\varepsilon_{s1}}{A_fE_f\varepsilon_f}\right) \approx N_{fad}\left(1 + \frac{A_{s1}E_s}{A_fE_f}\right) \tag{4.13}$$

Equation (4.13) was derived on the assumption that $\varepsilon_{s1}/\varepsilon_f \approx 1$.

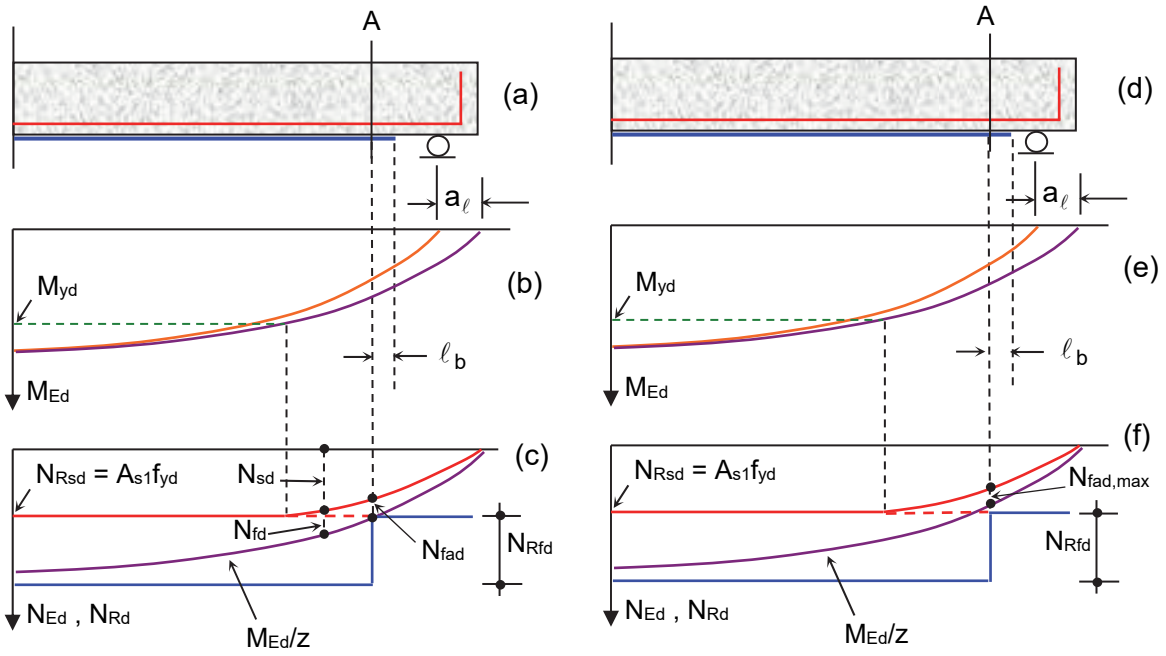

Fig. 4.6 Anchorage of FRP.

It is clear that the force N_{fad} is limited by $N_{fad,max}$ [eq. (3.3a), with safety factor γ_{fb}] and that sufficient space should be provided for the anchorage length ℓ_b. If this is not the case, section A must be re-positioned (in the direction where the bending moment decreases, that is towards the support), Fig. 4.6d-f, so that N_{fad} will be reduced to $N_{fad,max}$ or so that a lower ℓ_b will be required (as seen in Fig. 3.5, a small reduction in N_{fad} results in substantial reduction in ℓ_b). If the anchorage length is still not adequate, then the FRP width should be increased and the thickness decreased, or mechanical anchorages should be provided.

(5) Debonding at intermediate flexural crack

The analytical model described in Section 3.3 applies here too, provided that a proper correction is made to account for the fact that the true state of stress and strain at the concrete-FRP interface near vertical cracks in a real beam is not identical to that in the experimental setup of Fig. 3.2. Detailed finite element analyses as well as experimental evidence suggest that the maximum shear stress at the interface is much lower than the one found in the test setup. Based on the literature, it is proposed here to modify the model of Section 3.3.2 by increasing the debonding force by 150%. Hence,

the FRP strain corresponding to debonding in the vicinity of flexural cracks (where the shear force is practically zero) is calculated as follows:

$$\text{if } \ell_b \geq \ell_{b,max}: \quad \varepsilon_{fb,fl} = \frac{\alpha_{fl}}{\gamma_{fb}} \sqrt{\frac{0.6 f_{ctm} k_b}{E_f t_f}} \tag{4.14a}$$

$$\text{if } \ell_b < \ell_{b,max}: \quad \varepsilon_{fb,fl} = \frac{\alpha_{fl}}{\gamma_{fb}} \sqrt{\frac{0.6 f_{ctm} k_b}{E_f t_f}} \frac{\ell_b}{\ell_{b,max}} \left(2 - \frac{\ell_b}{\ell_{b,max}} \right) \tag{4.14b}$$

where $\alpha_{fl} = 2.5$.

The calculations for the resisting moment are performed as in the above case (2), with $\sigma_{fd} = E_f \varepsilon_{fb,fl}$.

(6) Debonding at intermediate shear crack

The statements made above apply here too, except that the increase of the debonding force is about 100% compared with the experimental values. Hence, the FRP strain corresponding to debonding in the vicinity of shear cracks is:

$$\text{if } \ell_b \geq \ell_{b,max}: \quad \varepsilon_{fb,fl-sh} = \frac{\alpha_{fl-sh}}{\gamma_{fb}} \sqrt{\frac{0.6 f_{ctm} k_b}{E_f t_f}} \tag{4.15a}$$

$$\text{if } \ell_b < \ell_{b,max}: \quad \varepsilon_{fb,fl-sh} = \frac{\alpha_{fl-sh}}{\gamma_{fb}} \sqrt{\frac{0.6 f_{ctm} k_b}{E_f t_f}} \frac{\ell_b}{\ell_{b,max}} \left(2 - \frac{\ell_b}{\ell_{b,max}} \right) \tag{4.15b}$$

where $\alpha_{fl-sh} = 2$.

The calculations for the resisting moment are performed as in the above case (2), with $\sigma_{fd} = E_f \varepsilon_{fb,fl-sh}$.

(7) FRP end shear failure – peeling-off

Investigations by several researchers (e.g. Oehlers 1992, Ziraba et al. 1994, Jansze 1997, Raoof and Hassanen 2000), have indicated that when externally bonded plates stop at a certain distance from the supports (as is typically the case in flexural strengthening applications) a nearly vertical crack might initiate at the plate end (plate end crack) and then grow as an inclined shear crack (Fig. 4.7). However, by virtue of internal stirrups, the shear crack may be arrested and the bonded-on plate separated from the concrete at the level of the longitudinal reinforcement in the form of spalling. The latter failure mode is also called concrete peeling-off, and is attributed to a critical

combination of shear and vertical tensile stresses at the plate end. A simple, yet reliable and conservative approach for the verification of FRP end shear failure involves the following checks:

$$V_{Ed,end} \leq 1.4 V_{Rd,c} \tag{4.16}$$

$$M_{Ed,end} \leq \frac{2}{3} M_{Rd} \tag{4.17}$$

where $V_{Ed,end}$ and $M_{Ed,end}$ is the acting shear force and bending moment (design values) at the FRP end, $V_{Rd,c}$ is the member shear resistance neglecting the contribution of stirrups and M_{Rd} is the moment resistance [minimum value calculated based on mechanisms (1), (2), (5) and (6)]. It is noted that the verification of eq. (4.17) is rather easy to achieve, e.g. by adjusting the FRP end. However, if eq. (4.16) is not satisfied, then the member should be strengthened near the FRP ends in shear (see next chapter).

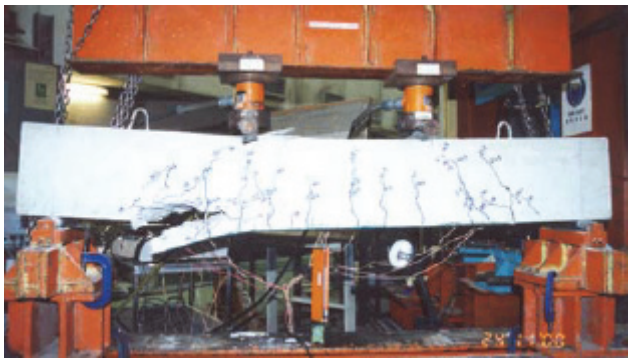

Fig. 4.7 FRP end shear.

4.5 Ductility considerations

The basic ductility requirement is to ensure activation of a failure mechanism that involves steel yielding, thereby securing a minimum curvature ductility factor (μ_ϕ). This implies that the tensile strain in the FRP at the ultimate limit state, $\varepsilon_{fu,c}$, must exceed a minimum value, $\varepsilon_{f,min}$; at the same time, this strain is limited by either the FRP ultimate strain (at fracture), ε_{fu}, or by the strain corresponding to debonding (but not necessarily at the critical cross section for flexural failure). Relevant to the above is Fig. 4.8.

The minimum FRP strain at the ultimate limit state, $\varepsilon_{f,min}$, corresponding to a given curvature ductility factor, μ_ϕ, is given as follows:

$$\varepsilon_{f,min} = \varepsilon_{yd} \frac{\mu_\phi}{\left(\frac{d}{h} - \frac{x_y}{h}\right)} - \varepsilon_{cu} - \varepsilon_o \tag{4.18}$$

where x_y is the neutral axis depth at yielding of the steel reinforcement.

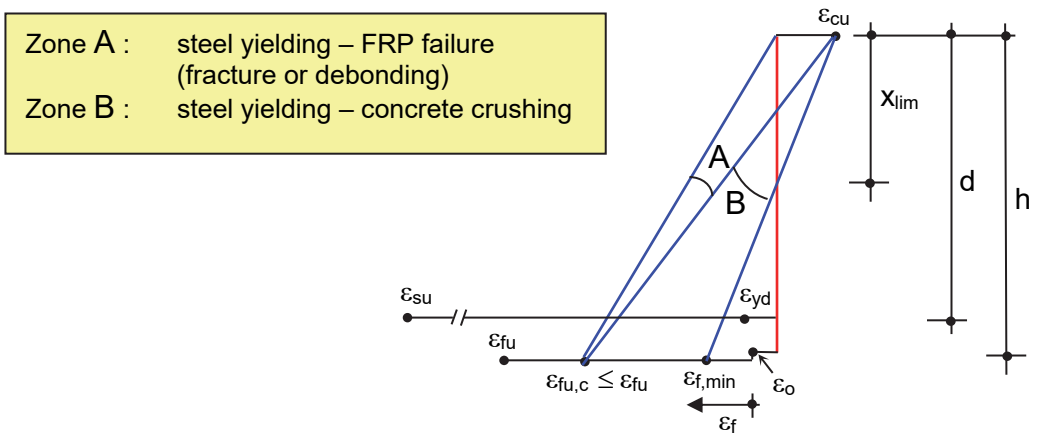

Fig. 4.8 Strain distribution at critical cross section.

A last point to be made here is that large ductility values are not always achievable, especially when the FRP quantity is controlled by serviceability, in which case the member is over-designed in terms of strength.

4.6 Summary of design calculations – ultimate limit state

A summary of the verifications for the ultimate limit state is provided next:

1. Determine the resisting moment for the member before strengthening ($M_{o,Rd}$).
2. From the service moment M_o prior to strengthening determine the initial strain ε_o at the extreme tension fiber.
3 Calculate the required FRP area A_f (corresponding to M_{Rd}) for cases (1), (2) and (6) [or (5), in the absence of shear force] at the critical section, based on eqs. (4.5)-(4.12). Note that these equations with $\varepsilon_c \le \varepsilon_{cu}$ and $\varepsilon_f \le \varepsilon_{f,lim} = \min(\varepsilon_{fu}, \varepsilon_{fb,fl-sh})$ describe three failure modes simultaneously (steel yielding – concrete crushing, steel yielding – FRP fracture, steel yielding – debonding at intermediate crack). As an approximation, $\varepsilon_{f,lim}$ may taken equal to 0.004-0.005. Next follows the ductility verification.
4. Calculate the anchorage length and finalize the FRP configuration based on the anchorage verification [mechanism (4)].
5. Verify failure mechanism (7) (FRP end shear failure). If not satisfied, shear strengthening is required (see next chapter).

6. Verify the shear resistance of the member (given that the flexural resistance has been increased). If not satisfied, shear strengthening is required.

4.7 Example

Consider the simply supported T-beam of Fig. 4.9 at a span of 5 m, under a uniformly applied vertical load of 65 kN/m. Materials: f_{cd} = 13.5 MPa, f_{ctm} = 2.2 MPa, f_{yd} = 435 MPa. Assuming an acting moment M_{Ed} = 203 kNm, design the appropriate strengthening system. Consider CFRP with thickness t_f = 1.1 mm, width 50 mm, elastic modulus E_f = 150 kN/mm^2 and ultimate strain (design value) ε_{fu} = 0.01. The service moment during strengthening is M_o = 47 kNm. Take γ_{Rd} = 1.

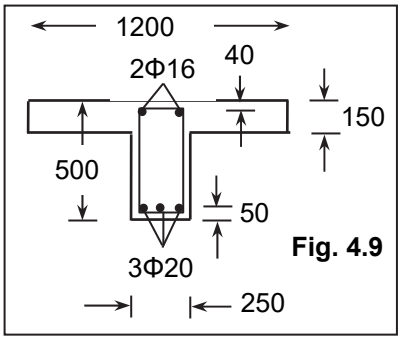

Fig. 4.9

Geometric data: A_{s1} = 940 mm^2, A_{s2} = 400 mm^2, h = 500 mm, d = 450 mm, d_1 = 50 mm, d_2 = 40 mm and b = 1200 mm. The ratio $\alpha_s = E_s / E_c$ equals 200/29 = 6.9. Solving eq. (4.1)-(4.4) we find ε_o = 0.00064.

Assuming $k_b \approx 1$, eq. (4.14a) for debonding near the mid-span (where the moment is maximum and the shear equals zero) gives:

$\varepsilon_{fb,fl} = \dfrac{2.5}{1.5}\sqrt{\dfrac{0.6 \times 2.2 \times 1.0}{150000 \times 1.1}} = 0.0047$, hence $\varepsilon_{f,lim}$ = min(0.01, 0.0047) = 0.0047, which is the FRP strain at the critical section (mid-span) for the ultimate limit state (debonding).

Next, with M_{Rd} = 203 kNm (and γ_{Rd} = 1) from eq. (4.5) – (4.12) we calculate x = 78 mm, ε_c = 0.00099 and A_f = 93 mm^2. Each strip has a cross section area equal to 55 mm^2, hence the use of <u>two strips</u> is required, with a total cross section area of 110 mm^2, which corresponds to M_{Rd} = 208.9 kNm, x = 79 mm and ε_c = 0.0010. These strips will be placed one next to the other, in order to avoid multiple layers.

The next step is the verification of the end anchorage (Fig. 4.10), which results in a total length of strips equal to 3.0 m.

Finally, the FRP end shear calculations give:

$$V_{Ed,end} = 65\left(\frac{5.00}{2} - 1.00\right) = 97.5 \text{ kN}, \quad M_{Ed,end} = 65 \times 1.00 \times \left(\frac{5.00}{2} - \frac{1.00}{2}\right) = 130 \text{ kNm}$$

Suppose $V_{Rd,c}$ = 40 kN, hence 1.4x40 = 56 kN.

It is concluded that (4.17) is satisfied (2x208.9/3 > 130) but (4.16) is violated, hence the ends should be strengthened in shear for a shear force equal to 97.5 – 56 = 41.5 kN (according to the procedure described in Chapter 5).

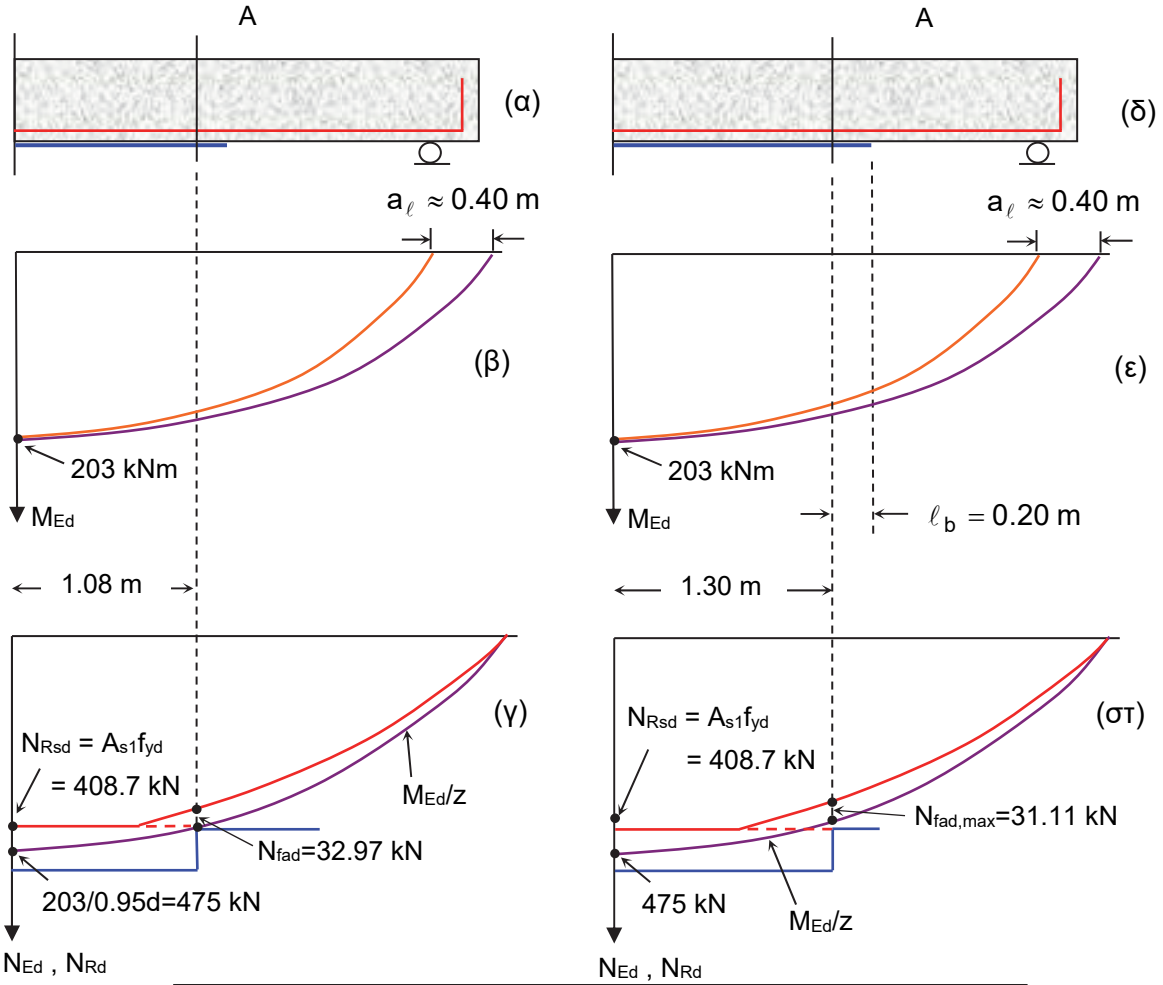

$$408.7 \approx N_{fad}\left(1+\frac{940\times 200}{110\times 150}\right) \Rightarrow N_{fad} = 32.97 \text{ kN}$$

$$N_{fad,max} = \frac{100}{1.50}\sqrt{0.6\times 1.0\times 150000\times 2.2\times 1.1}\times 10^{-3} = 31.11\,\text{kN}$$

$$\ell_{b,max} = 0.6\sqrt{\frac{150000\times 1.1}{\sqrt{2.2}\times 1.0}} = 200.1\,\text{mm} \rightarrow 0.20\text{ m}$$

Fig. 4.10 Verification of anchorage.

4.8 Servicability limit state

Calculations to verify the serviceability limit state may be performed according to a linear elastic analysis and considering that the concrete does not sustain tension (Fig. 4.11).

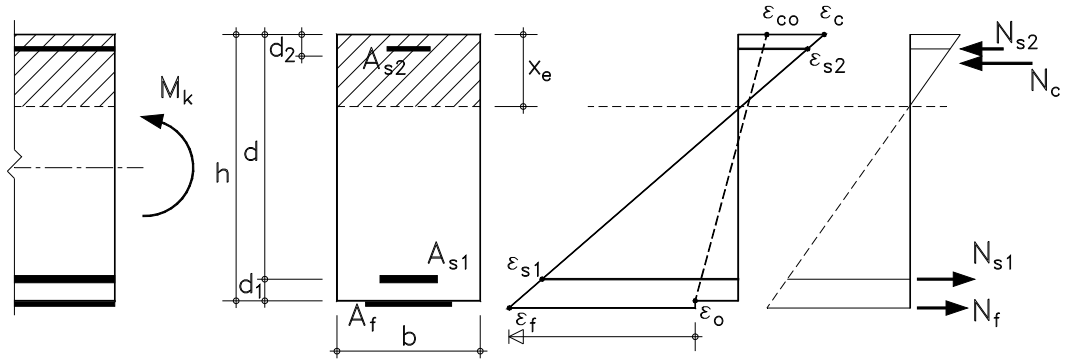

Fig. 4.11 Linear elastic analysis of cracked section.

From the equilibrium of forces and strain compatibility, the depth of the neutral axis x_e is obtained from the following:

$$\frac{1}{2}bx_e^2+(\alpha_s-1)A_{s2}(x_e-d_2)=\alpha_s A_{s1}(d-x_e)+\alpha_f A_f\left[h-\left(1+\frac{\varepsilon_o}{\varepsilon_c}\right)x_e\right] \tag{4.19}$$

$$E_c\varepsilon_c=\frac{M_k}{\frac{1}{2}bx_e\left(h-\frac{x_e}{3}\right)+(\alpha_s-1)A_{s2}\frac{(x_e-d_2)}{x_e}(h-d_2)-\alpha_s A_{s1}\frac{d-x_e}{x_e}(h-d)} \tag{4.20}$$

where $\alpha_f=E_f/E_c$ and M_k is the characteristic value of the acting moment. The last two equations can be solved for the unknown x_e and ε_c.

The moment of inertia of the cracked section is given by:

$$I_2=\frac{bx_e^3}{3}+(\alpha_s-1)A_{s2}(x_e-d_2)^2+\alpha_s A_{s1}(d-x_e)^2+\alpha_f A_f(h-x_e)^2 \tag{4.21}$$

whereas that of the uncracked section may be approximated as follows (for rectangular cross sections):

$$I_1\approx\frac{bh^3}{12} \tag{4.22}$$

Regarding **stress** verification, apart from limiting stresses in the concrete and steel, it is required to limit the stress in the FRP, σ_f, under the rare load combination, as follows:

$$\sigma_f=E_f\left(\varepsilon_c\frac{h-x_e}{x_e}-\varepsilon_o\right)\le\eta f_{fk} \tag{4.22}$$

where the reduction coefficient $\eta < 1$ accounts for the poor behavior of some composites (e.g. GFRP) under sustained loading. Based on creep rupture tests (e.g. Yamaguchi et al. 1998), indicative values of η are 0.8, 0.5 and 0.3 for CFRP, AFRP and GFRP, respectively. Note that as the design is often governed by the serviceability limit state, relative low FRP strains at service load may be expected, so that FRP creep rupture is typically not of concern.

The verification of **deflections** and **crack widths** is performed in analogy to the case of reinforced concrete members (e.g. *fib* 2001).

4.9 Columns

The analysis of cross sections where bending develops in combination with an axial force is performed according to the principles presented above, the basic difference being the addition of one more term in the force and moment equilibrium equations: N_{Ed} in the right part of eq. (4.5) and $N_{Ed}[(h/2)-\delta_G x]$ in the right part of eq. (4.8), where N_{Ed} is the acting axial force (design value). Furthermore, the contribution of FRP in carrying compression should be neglected. Assuming that debonding is prevented (e.g. through proper anchorage inside slabs or joints, Fig. 4.2b-c, the failure mechanism will be one of the following:

- yielding of tension steel ($\varepsilon_{s1} \geq f_{yd}/E_s$), concrete crushing ($\varepsilon_c = \varepsilon_{cu}$)
- yielding of tension steel ($\varepsilon_{s1} \geq f_{yd}/E_s$), debonding or FRP fracture [$\varepsilon_f = \varepsilon_{f,lim} = \min(\varepsilon_{fu}, \varepsilon_{fb,fl-sh})$]
- concrete crushing ($\varepsilon_c = \varepsilon_{cu}$)

The bending moment – axial force interaction at failure is best demonstrated through the so-called interaction diagrams, such as those given in Fig. 4.12a-b. Those diagrams have been constructed for various equivalent geometric ratios of steel and FRP reinforcement, ρ_{eq}, defined as:

$$\rho_{eq} = \rho_s + \rho_f \frac{E_f}{E_s} = \frac{A_{s,tot}}{bd} + \frac{A_{f,tot}}{bd}\frac{E_f}{E_s} \tag{4.23}$$

where $A_{s,tot} = 2A_{s1} = 2A_{s2}$ (symmetrically placed steel reinforcement) and $A_{f,tot} = 2A_f$ (symmetrically placed FRP reinforcement). Moreover, for the sake of simplicity it has been assumed that $\varepsilon_{f,min}$=0.008.

The interaction diagrams in Fig. 4.12 show that the effectiveness of FRP in increasing the flexural capacity decreases substantially as the axial load increases.

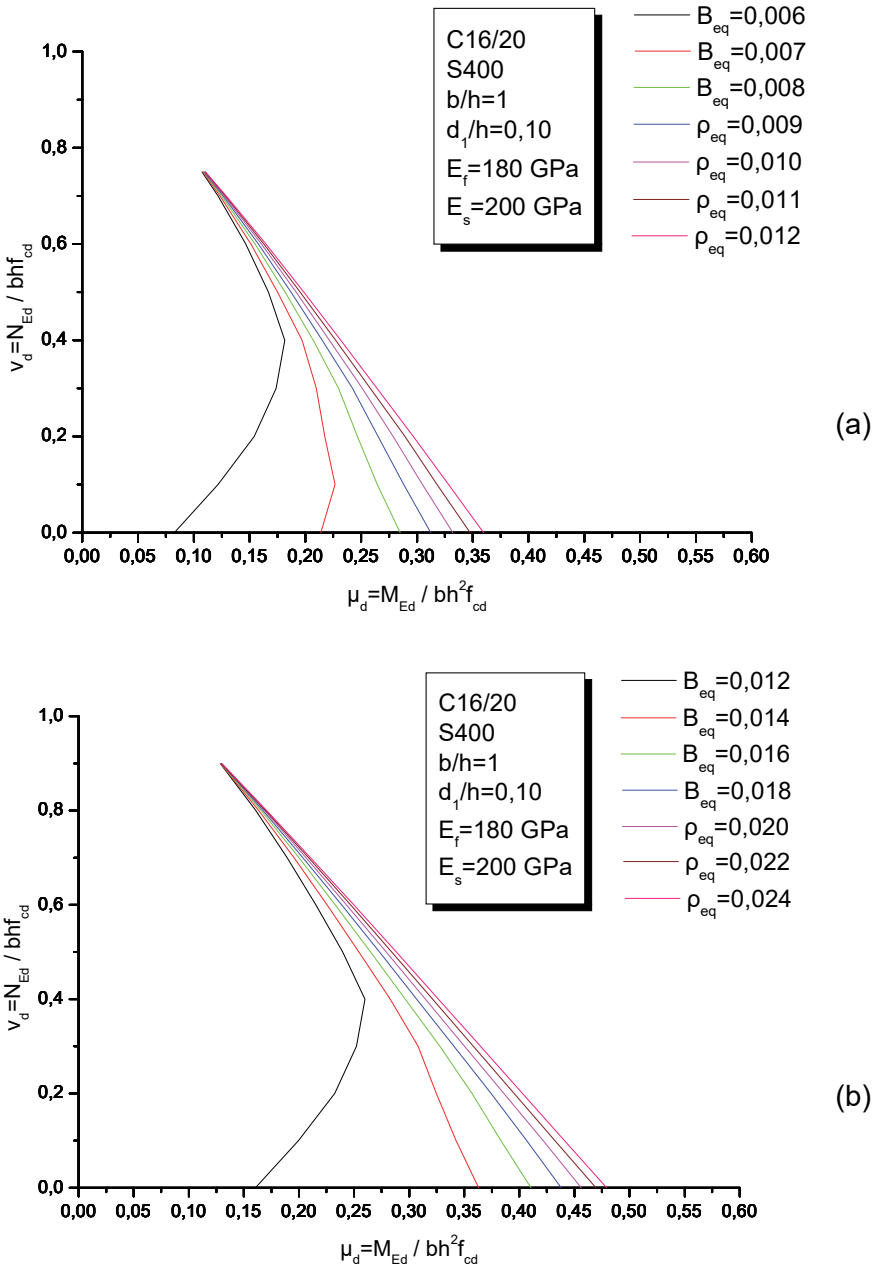

Fig. 4.12 Axial force – bending moment interaction diagrams for square cross sections (b=h) under uniaxial bending. Concrete C16/20, steel S400, $d_1/h=0.10$, E_f =180 kN/mm^2. (a) $A_{s,tot}=0.006$, (b) $A_{s,tot}=0.012$.

As a general conclusion one may state that flexural strengthening of columns is not always feasible (and easy as in the case of beams); and certainly the FRP contribution is of rather low effectiveness, unless the axial load is kept at low levels (e.g. ν_d < 0.2).